

Optimized Conditions for the Self-Organization of CdSe-Au and CdSe-CdSe Binary Nanoparticle Superlattices

Chenguang Lu,[†] Zhuoying Chen,[†] and Stephen O'Brien*

Materials Science and Engineering Center and Department of Applied Physics and Applied Mathematics, Columbia University, New York, New York 10027

Received October 31, 2007. Revised Manuscript Received February 23, 2008

The formation process of CdSe-Au binary nanoparticle superlattices (BNSLs) was investigated to elucidate the optimal conditions for self-assembly. Nanoparticle mixtures were prepared under suitable and variable solvent evaporation conditions and the products analyzed by TEM. 1-Dodecanethiol was found to be critical for superlattice formation, prior to the onset of short-range nanoparticle–nanoparticle interactions that likely dictate structure, highlighting the multiple roles of this organic polar molecule as both a ligand that coats the particle during synthesis and then as a high boiling point/crystallization solvent for the separate step of BNSL formation. The influence of 1-dodecanethiol was investigated under various concentrations to determine optimized conditions for guided assembly, for which relatively large ($>1\ \mu\text{m}^2$) areas of superlattices could be routinely formed. Depending on appropriate selection of the radius ratio, AB or AB₅ binary structures of CdSe-Au nanoparticles were generated. The optimized conditions for the CdSe/Au binary nanoparticle system was applied to, and found to be equally effective for, a binary mixture of CdSe/CdSe. We characterize CdSe-Au and CdSe-CdSe as additional systems to the library of possible BNSLs.

Introduction

Self-assembly, one of the core concepts in nanotechnology, is being studied and explored in many areas.^{2–11} In general, this approach attempts to take advantage of favorable thermodynamic driving forces (entropic, enthalpic, or both) to guide in the formation of ordered and functional macroscopic structures. The merits of the approach are low power consumption, low cost, and ease of generating nanoscopic features compared with, for example, top-down photolithographic techniques used in Integrated Device Manufacturing. The self-assembly of nanoparticles of two different materials into a binary nanoparticle superlattice (BNSL) can provide a general pathway to a large variety of materials with precisely controlled chemical composition and tight placement of the components.¹² Establishing the conditions

necessary for the preparation of binary nanoparticle superlattices requires assessment of a wide variety of chemical and thermodynamic parameters that contribute to the overall process. Previously it has been observed that, in addition to entropy, van der Waals, steric, and dipolar forces,¹³ electrical charges on sterically stabilized nanoparticles can determine BNSL stoichiometry, and this phenomenon is not limited to one length scale.^{12,14–16}

Here, we investigate the sensitivity of BNSL formation to ligand concentration in a high boiling point–low boiling point mixed solvent system (thiol–toluene) and report the preparation of superlattices containing two sizes of monodisperse nanoparticles of cadmium selenide–gold (CdSe-Au) and cadmium selenide (CdSe-CdSe). Conditions were varied and optimized for the formation of a BNSL based on AB and AB₅ structures.¹⁷ We found that excess thiol acts as a high boiling point solvent critical for the formation of islands on the substrate suitable for BNSL nucleation and growth. This occurs long after the low boiling point solvent, toluene, evaporates. BNSL formation is found to be contingent on sufficient thiol present to create a ratio of 2.5:1 with respect to the high boiling point solvent:nanoparticle volume

* Corresponding author. E-mail: so188@columbia.edu.

[†] These authors contributed equally to this work.

- (1) Yin, M.; Chen, Z. Y.; Deegan, B.; O'Brien, S. J. *Mater. Res.* **2007**, *22* (7), 1987–1995.
- (2) Hawker, C. J.; Russell, T. P. *MRS Bull.* **2005**, *30* (12), 952–966.
- (3) Keren, K.; Berman, R. S.; Buchstab, E.; Sivan, U.; Braun, E. *Science* **2003**, *302* (5649), 1380–1382.
- (4) Talapin, D. V.; Murray, C. B. *Science* **2005**, *310* (5745), 86–89.
- (5) Sun, S. H.; Murray, C. B.; Weller, D.; Folks, L.; Moser, A. *Science* **2000**, *287* (5460), 1989–1992.
- (6) Murray, C. B.; Kagan, C. R.; Bawendi, M. G. *Science* **1995**, *270* (5240), 1335–1338.
- (7) Urban, J. J.; Talapin, D. V.; Shevchenko, E. V.; Kagan, C. R.; Murray, C. B. *Nat. Mater.* **2007**, *6* (2), 115–121.
- (8) Cheon, J.; Park, J. I.; Choi, J. S.; Jun, Y. W.; Kim, S.; Kim, M. G.; Kim, Y. M.; Kim, Y. J. *Proc. Natl. Acad. Sci. U.S.A.* **2006**, *103* (9), 3023–3027.
- (9) Tang, Z. Y.; Zhang, Z. L.; Wang, Y.; Glotzer, S. C.; Kotov, N. A. *Science* **2006**, *314* (5797), 274–278.
- (10) Manna, L.; Scher, E. C.; Alivisatos, A. P. *J. Am. Chem. Soc.* **2000**, *122* (51), 12700–12706.
- (11) Liang, H. J.; Whited, G.; Nguyen, C.; Stucky, G. D. *Proc. Natl. Acad. Sci. U.S.A.* **2007**, *104* (20), 8212–8217.

- (12) Shevchenko, E. V.; Talapin, D. V.; Kotov, N. A.; O'Brien, S.; Murray, C. B. *Nature* **2006**, *439* (7072), 55–59.
- (13) Talapin, D. V.; Shevchenko, E. V.; Murray, C. B.; Titov, A. V.; Kral, P. *Nano Lett.* **2007**, *7* (5), 1213–1219.
- (14) Leunissen, M. E.; Christova, C. G.; Hynninen, A. P.; Royall, C. P.; Campbell, A. I.; Imhof, A.; Dijkstra, M.; van Roij, R.; van Blaaderen, A. *Nature* **2005**, *437* (7056), 235–240.
- (15) Bartlett, P.; Campbell, A. I. *Phys. Rev. Lett.* **2005**, *95* (12), 128302.
- (16) Kalsin, A. M.; Fialkowski, M.; Paszewski, M.; Smoukov, S. K.; Bishop, K. J. M.; Grzybowski, B. A. *Science* **2006**, *312* (5772), 420–424.
- (17) Shevchenko, E. V.; Talapin, D. V.; Murray, C. B.; O'Brien, S. J. *Am. Chem. Soc.* **2006**, *128* (11), 3620–3637.

Table 1. Nanoparticle/Thiol Ratios in Figure 1

	solvent conditions (% thiol volume in toluene)	estimated nanoparticle/ thiol volume ratio	morphologies of nanoparticle mixture after drying
Figure 1a,b Figure 1c,d	no xs thiol 0.1 (0.004 mol/L)	no xs thiol 0.05	nanoparticles spreading over the surface low level of clustering of nanoparticles while most nanoparticles spread over the surface
Figure 1e,f Figure 1g,h	0.6 (0.026 mol/L) 3.8 (0.16 mol/L)	0.0083 0.0014	BNSL formation <8 h nanoparticles clustering and some BNSL formation >24 h

ratio. BNSL formation does not occur unless sufficient ligand is present, but an excess can cause the system to be “too oily” for BNSLs to form in a reasonable time domain.

Although dozens of structures have been shown to be possible,^{12,18–20} many issues yet reside in the path toward making functional BNSLs on a range of substrates and to specifications desirable for optical, electronic, or magnetic characterization, with a view toward device creation. By using 1-dodecanethiol/toluene as a solvent, semiconductor–metal BNSL films, up to $1 \mu\text{m}^2$, can routinely and ubiquitously form on amorphous carbon films of a TEM grid. This technique furthers the ability to make large areas of BNSL films for possible applications and fundamental studies, such as solar cell photovoltaics, charge transport devices, and optoelectronic materials.

Methods

Reagents (Aldrich) were used as purchased. CdSe nanoparticle synthesis: typically, 102.8 mg of CdO, 910 mg of stearic acid, and 32 mL of octadecene were mixed in a 120 mL three-necked flask. The mixture was heated at 250 °C for 10 min to allow the formation of cadmium stearate. Then 4 g of trioctylphosphine oxide and 4 g of octadecylamine were added followed by degassing. After the mixture was then heated to 300 °C, a 4 mL solution of 1.0 M trioctylphosphine selenide in trioctylphosphine was injected quickly. The growth was carried out at 270 °C. Injection and growth temperatures were varied to obtain differently sized CdSe nanoparticles.²¹ The product was purified with ethanol/toluene. Au nanoparticle synthesis: Brust's method²² was modified with a digestive ripening process²³ to increase size monodispersity. Typically 34 mg of gold chloride, 92.5 mg of didodecyltrimethylammonium bromide, and 10 mL of toluene were mixed by sonication. The solution was stirred vigorously, into which 40 μL of 9.4 M NaBH_4 in water solution was injected. After 15 min, 800 μL 1-dodecanethiol was added followed by another 5 min of stirring. The product was purified by an ethanol/toluene solvent pair and finally dispersed in 10 mL of toluene and 800 μL of 1-dodecanethiol mixture. The solution was refluxed for 30 min. The final product was purified with an ethanol/toluene solvent pair and dispersed in toluene. Samples were analyzed by TEM (JEOL 100cx). All grids were 200 mesh amorphous carbon backed copper (EMS). The amount of 1-dodecanethiol was varied to study its effect on BNSL formation. The samples were first dried in ambient conditions for 24 h and then put in a RT vacuum chamber for further

drying. All images shown in the figures are from representative areas of the samples.

To prepare the BNSL, a TEM grid was put into a test tube with 40 μL of a CdSe/Au nanoparticle mixture in toluene. The Au:CdSe nanoparticle ratio was varied from 1:10 to 10:1 in an attempt to obtain different BNSL symmetries for a given size ratio. For example, preference for the AB_2 structure was observed for a particle mixture of 1:2 Au:CdSe. The ratio between numbers of Au and CdSe particles in their original solutions was estimated as follows: Two dispersions of Au and CdSe nanoparticles were mixed. Necessary dilution of the mixture was performed to achieve clear and countable nanoparticles by TEM. By assuming that the two solutions were mixed homogeneously, one can assume that the numbers of Au and CdSe presenting on the same area are representative of the entire mixture. The numbers of Au and CdSe nanoparticles were counted (e.g., 100 CdSe and 50 Au) and verified on other sections of the grid. This empirically derived ratio was used as a guideline for the molar concentration ratio and cross-referenced with the molar starting quantities. Absolute concentration of the original Au nanoparticle solution was determined by TGA. Complete removal of organic is assumed to occur >600 °C. Using the residual weight (e.g., 0.025 mg per 25 μL of original solution), using Au's bulk density, the total volume can be obtained (e.g., $1.3 \times 10^{-3} \mu\text{L}$ Au per 25 μL of original solution) to give a volume fraction (5.2×10^{-5}). This value was used to calculate a ratio between particle volume and extra solvent (thiol) volume provided in Table 1.

To monitor the solvent evaporation during BNSL formation, a TGA pan was used to contain the TEM grid with 40 μL of binary CdSe and Au solution (1:5 ratio). After 12 h in air at room temperature (most of the toluene evaporated during this 12 h), this TGA pan containing the TEM grid was put into a TGA instrument and the instrument was set to constant 65 °C under a N_2 flow for 8 h.

Results and Discussion

The thermodynamic driving forces for assembly of nanoparticles into superlattices are currently understood in terms of a delicate interplay between entropic, possible Coulombic, charge–dipole, dipole–dipole, and dispersive (London–van der Waals) interactions between the nanoparticles.^{12,16,24} It was observed under certain conditions that electrical charges on the nanoparticles can be influenced by the addition of capping ligands during the drying the process, based on electrophoretic mobility measurements of PbSe and Au nanoparticles in the presence of trioctylphosphine oxide and oleic acid in chloroform, and that Coulomb interactions might contribute to the lattice stabilization energy of the superlattice. We have recently postulated that favorable ligand–ligand interactions (van der Waals forces) may also play a signifi-

(18) Shevchenko, E. V.; Talapin, D. V.; O'Brien, S.; Murray, C. B. *J. Am. Chem. Soc.* **2005**, *127* (24), 8741–8747.

(19) Saunders, A. E.; Korgel, B. A. *ChemPhysChem* **2005**, *6* (1), 61–65.

(20) Kiely, C. J.; Fink, J.; Zheng, J. G.; Brust, M.; Bethell, D.; Schiffrin, D. J. *Adv. Mater.* **2000**, *12* (9), 640.

(21) Peng, Z. A.; Peng, X. G. *J. Am. Chem. Soc.* **2001**, *123* (1), 183–184.

(22) Brust, M.; Walker, M.; Bethell, D.; Schiffrin, D. J.; Whyman, R. *J. Chem. Soc., Chem. Commun.* **1994**, (7), 801–802.

(23) Stoeva, S.; Klabunde, K. J.; Sorensen, C. M.; Dragieva, I. J. *Am. Chem. Soc.* **2002**, *124* (10), 2305–2311.

(24) Chen, Z.; Moore, J.; Radtke, G.; Sirringhaus, H.; O'Brien, S. *J. Am. Chem. Soc.* **2007**, *129* (50), 15702–15709.

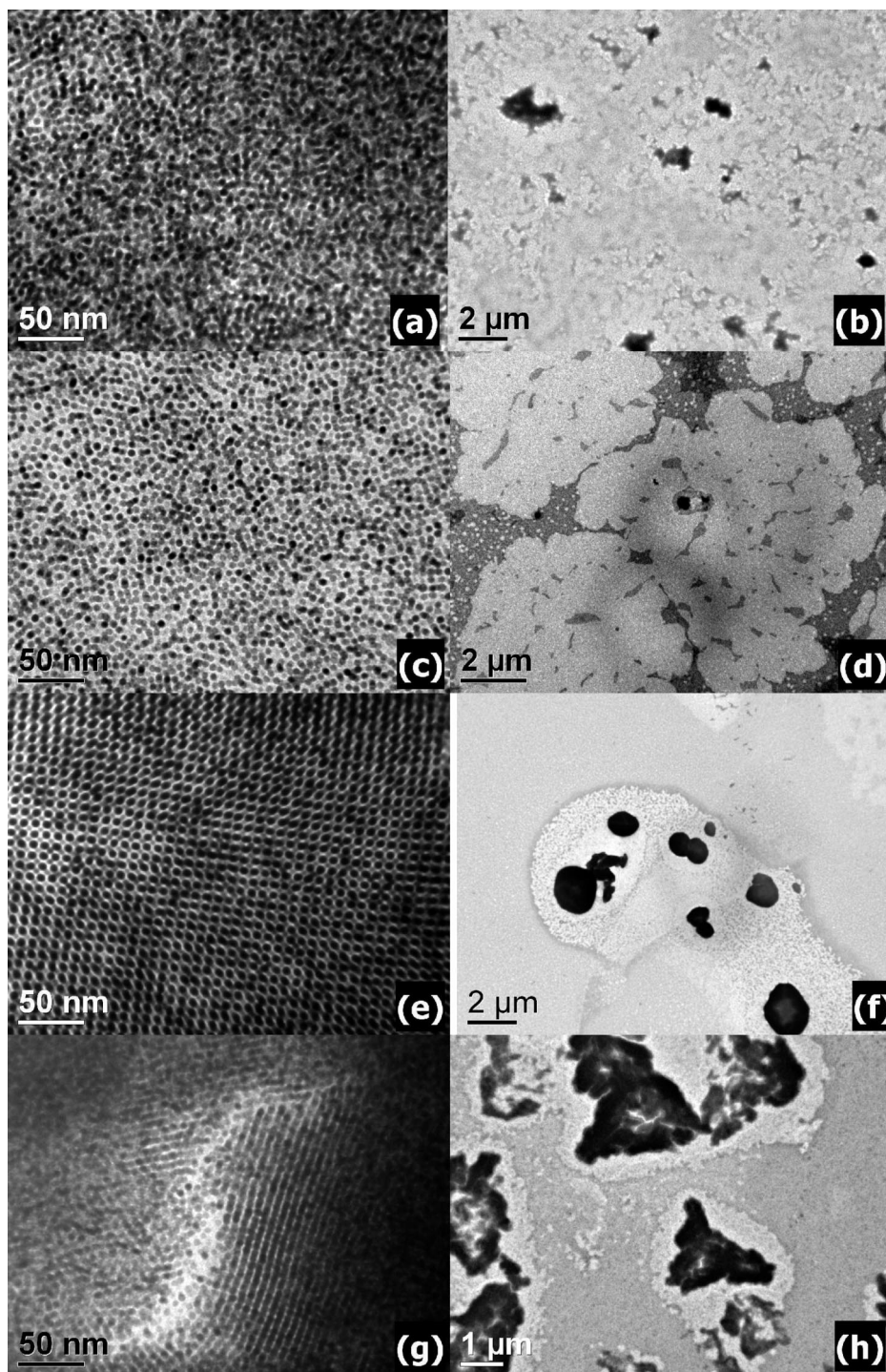


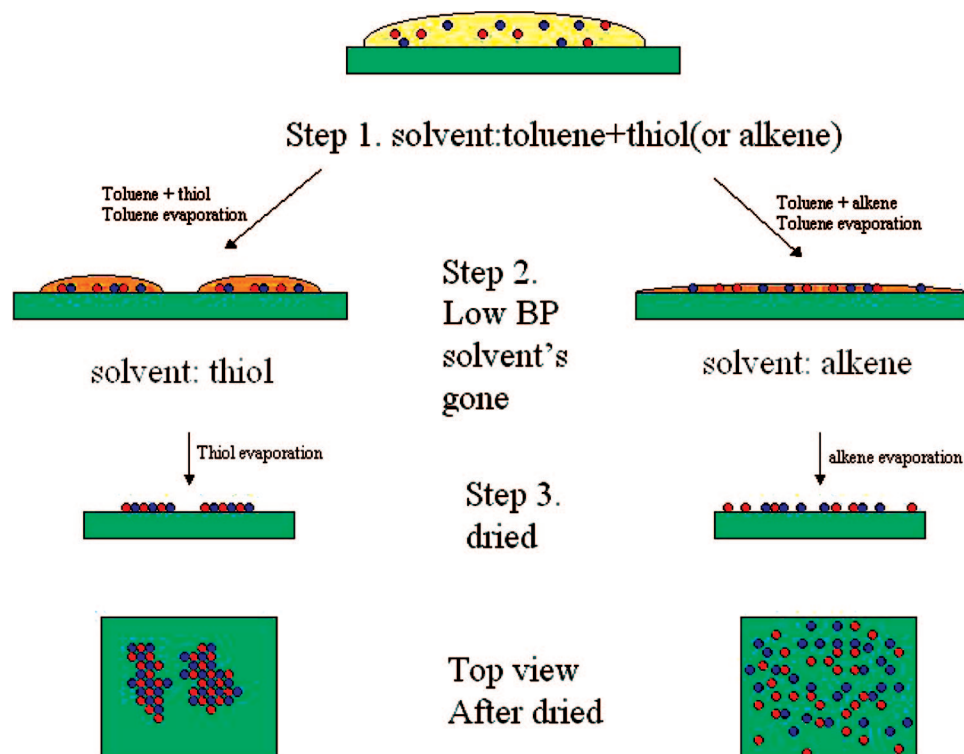
Figure 1. High (left column) and low (right column) magnification TEM images of 3.5 nm CdSe and 5.0 nm Au nanoparticle mixtures with increasing amounts of thiol present after solvent evaporation. Initial thiol/toluene ratios: (a, b) zero; (c, d) 0.1%; (e, f) 0.6%; (g, h) 3.8%. The structure of BNSLs is the CuAu alloy structure.

cant role in contributing to the lattice stabilization energy.²⁴ Because of the large range of nanoparticle materials available, for example, semiconductors of different crystal symmetries or metals that may pick up charge, it is currently difficult to conclude with certainty one overall formation mechanism. However, it is no surprise that conditions necessary for the onset of these interparticle forces to drive assembly are strongly reliant on experimental parameters such as drying conditions, vapor pressures, and solvent evaporation rates. The focus here is with improving the appropriate microscopic conditions for the assembly of CdSe-

Au superlattices as a model system and as an extension to all semiconductor-metal or semiconductor-semiconductor BNSLs.

Figure 1 shows the structure of CdSe (3.5 nm) and Au (5 nm) nanoparticles mixture (1:1 particle ratio, optimized for AB symmetry) on carbon film backed TEM grids. At low thiol concentrations ($>0.63\%$ volume ratio of thiol in toluene), the two types of nanoparticles mixed well but no ordered structure was found. For $>0.63\%$ or more volume ratio of thiol in toluene, the AB superlattice formed. We compared low magnification TEM images of these samples

Scheme 1. Proposed Drying Behaviors of Thiol/Toluene and Octadecene/Toluene Mixtures on Nanoparticle Assemblies



as shown in Figure 1. Generally, islands of low electron beam transparency are where BNSL are found to form, appearing as dense dark circular regions. Nanoparticles are seen to cluster together to form islands in samples with higher thiol concentrations. For low thiol concentrations, these islands are not visible and the distribution of nanoparticles is more uniform across the substrate. Table 1 summarizes the relationship between estimated nanoparticle/thiol volume ratios and the final morphologies of binary nanoparticle mixtures after complete drying. The volume ratio is based on an estimation of (i) the concentration of nanoparticles in the mixture (determined by wt % from TGA analysis), (ii) the volume of an individual nanoparticle from the diameter (TEM), and (iii) the concentration of thiol initially present in the solution primed for BNSL formation. The actual volume ratio between nanoparticles and thiol may differ, since many nanoparticles are not confined in the thiol droplets and a large portion of thiol may also settle outside. The values in this table therefore remain an empirical estimation for optimized conditions for BNSL formation.

Due to the volatility difference during the drying process, toluene evaporates first with 1-dodecanethiol forming droplets on the substrate before its subsequent evaporation: toluene (boiling point 110 °C) and 1-dodecanethiol (boiling point >250 °C). The weight loss of a partially dried sample was monitored by TGA at 65 °C over an 8 h period, a period that extends into the time required for BNSL formation (Supporting Information, Figure 1). During the first 33 min there is a significant weight drop due to the removal of residual toluene. After that, 1-dodecanethiol is believed to be evaporating continuously and slowly, giving rise to a decline in weight. The system maintained approximately the same drying speed >8 h. The total weight loss for the “free” thiol for this 8 h period was determined to be around

0.004416 mg, measured from the weight difference between 33 and 480 min. It is assumed that BNSLs that have formed have done so with the elimination of thiol after this time. The original capping ligands for the Au are 1-dodecanethiol, but for CdSe they are predominantly octadecyl amine, with some limited trioctyl phosphine or phosphine oxide also present.²⁴ It is conceivable that ligand exchange could occur during the drying process and some of the xs 1-dodecanethiol substitutes as the surface ligand on the CdSe nanoparticles. These results suggest that free excess ligand, such as thiols or long chain carboxylic acids typically used in the nanoparticle synthesis procedure, act as a high boiling point solvent responsible for aiding in the self-organization of nanoparticles to form superlattices. The nanoparticles are confined to these slowly evaporating droplets, which further drives the nanoparticles together into an increasingly shrinking volume (saturated solution) until a critical nucleation point. Scheme 1 is a representation of this self-organization process. In samples without thiol, no BNSL was observed. At higher concentration of thiol, drying times were prolonged: 3.8% thiol/toluene solvent always took longer times (>1 week) to form superlattices versus those in the 0.63% thiol/toluene solvent regime (>24 h). We conclude BNSL formation occurs during evaporation of thiol, and there is an ideal ratio of thiol/toluene (in this case ~1/100 by volume) for the optimized formation of the AB CdSe-Au BNSL.

It is also apparent from these and previous findings¹⁶ that BNSL formation is sensitive to substrate wetting in addition to and concurrent with solvent concentration/drying conditions. It has been postulated that free electrons in conducting carbon substrates affect the crystallization process through dielectric screening of the nanoparticle charges.¹² In this study we confine ourselves to exploring the role of the solvent and solvent polarity on a consistent and uniform

Table 2. Summary of Effects of Solvent on BNSL Formation

low boiling point solvent	high boiling point solvent	nanoparticle species	final nanoparticle assemblies	symmetry if BNSL formed
toluene	dodecanethiol	CdSe/Au, CdSe/CdSe	BNSLs clustering into nanoparticle islands	AB, AB ₅
	oleic acid ^a	Fe ₃ O ₄ /Au		AB ₂
	trioctyl phosphine oxide ^b	PbSe/Au, PbSe/Ag, PbSe/Pd	unknown	AB ₁₃ , AB ₅
	octadecene	CdSe/Au	nanoparticles spreading out, short-range ordering of nanoparticles	none identified
	tetradecene	CdSe/Au		

^a From ref 1 and laboratory work. ^b From ref 12.

hydrophobic amorphous carbon substrate. We have other high boiling point solvents with notably different physical characteristics in BNSL formation, and the results are summarized in Table 2 together with references. BNSLs generally form in polar high BP solvents and not in nonpolar solvents. For example, octadecene fringes, indicative of small areas of periodicity, can be observed with low magnification TEM, but it is unclear if these structures are BNSLs (Supporting Information, Figure 3). The different drying patterns suggest that solvent polarity plays a role, which could be due either to substrate wetting or to dielectric screening of the particles. For the case of octadecene a lower wetting contact angle and therefore inability to form droplets on the substrate would potentially inhibit the assembly process. Such an observation supports claims that confinement of particles to a shrinking volume is necessary to create close packed structures driven by entropic forces.^{24,25} We conclude that on this substrate, polar solvents such as thiol, oleic acid, and TOPO can be used for BNSL formation, whereas nonpolar alkenes do not aid in the formation of large area BNSLs. Dielectric screening may also be an important parameter to consider for the modeling of interparticle forces, especially if charge on the particles has occurred.¹² The Hamaker constant, A , is required for examining the approach of two nanoparticles screened by a hydrocarbon layer. For example, $A \sim 0.3$ eV for a CdSe/hexane/CdSe system. The Hamaker values are mainly dependent on the material, but additional consideration to the nature of the solvent layer may be necessary for fine calculations, and alkane thiols are typically in possession of higher A than n -alkanes by $\sim 20\%$.²³

Following the assumption that confinement of the nanoparticles into a shrinking volume is critical for BNSL formation, we wished to determine whether or not the structures favored by the formation process can be rationalized as close packed structures. The BNSL shown in Figure 2a is composed of CdSe nanoparticles of average diameter 6.8 nm and Au of average diameter 6 nm. This BNSL structure is isostructural with the AuCu structure. The thickness of the organic ligand shell of the CdSe and Au nanoparticles is measured to be around 0.8 and 0.7 nm, respectively (Supporting Information, Figures 4 and 5). The effective diameter of the nanoparticle components is equal to the sum of the crystal core and twice the thickness of the ligand shell. Therefore, the effective size ratio γ is ~ 0.88 . Using the hard-sphere packing model and considering the effective volume of all the nanoparticle components within a unit cell and the unit cell dimension (measured by TEM

in different orientations, $a \sim 12.2$ nm and $c \sim 10.4$ nm in this case), the hard-sphere packing density can be determined to be around 0.68. Figure 2b shows another AuCu structure BNSL composed of 3.5 nm CdSe (effective 5.1 nm) and 5.0 nm Au (effective 6.4 nm). The effective size ratio γ of this CdSe-Au pair is around 0.8. The AB₅ structure (Figure 2e) is composed of CdSe of average diameter 6.8 nm (effective 8.4 nm) and Au of average diameter 5.8 nm (effective 7.2 nm). This gives an effective size ratio ~ 0.85 . The unit cell dimension of this AB₅ BNSL is measured to be $a \sim 14.3$ nm and $c \sim 10.2$ nm. The hard-sphere packing density of this AB₅ structure determined by the same method is ~ 0.61 . On the basis of the hard-sphere model, neither of the packing densities of these BNSLs with their specific size ratios described exceed the packing densities of single component close-pack structures (e.g., fcc or hcp, packing density 0.74). We have observed similar effects previously for the formation of CdSe-CdTe superlattices and concluded that ligand–ligand interactions play a role in structure direction.²⁴ Over the range of tested conditions for the CdSe-Au BNSL systems prepared, “clustering” of the nanoparticles was frequently observed regardless of the size ratio of the nanoparticle pair and symmetry of the superlattice. Such an observation strongly suggests attractive forces between nanoparticles, and a Coulombic pairwise interaction might be an explanation given that metal particles have been shown to adopt a negative charge, while the semiconductor can adopt a positive charge.^{12,16} For the formation of CdSe-Au BNSLs we conclude that an optimized space filling geometry is adopted as a consequence of self-organization of the nanoparticles, but the precise nature of the interparticle interaction continues to require further investigation.

Previous research on evaporation mediated self-assembly of nanoparticles has indicated that nanoparticles possess great mobility in the solution phase and can be ordered under optimized conditions.^{6,26–31} However, there is still a lack of understanding on the details of events that lead to a particular style of ordering during the final stages of solvent evaporation.⁶ Our results suggest that a binary solvent mixture with optimized amounts of high boiling point solvent could possibly prolong the time scale needed for nanoparticles to settle. In cases of fast evaporation of the solvent, “Coffee

(25) Eldridge, M. D.; Madden, P. A.; Frenkel, D. *Nature* **1993**, 365 (6441), 35–37.

(26) Rabani, E.; Reichman, D. R.; Geissler, P. L.; Brus, L. E. *Nature* **2003**, 426 (6964), 271–274.

(27) Xu, J.; Xia, J. F.; Lin, Z. Q. *Angew. Chem., Int. Ed.* **2007**, 46 (11), 1860–1863.

(28) Bigioni, T. P.; Lin, X. M.; Nguyen, T. T.; Corwin, E. I.; Witten, T. A.; Jaeger, H. M. *Nat. Mater.* **2006**, 5 (4), 265–270.

(29) Ge, G. L.; Brus, L. J. *Phys. Chem. B* **2000**, 104 (41), 9573–9575.

(30) Tang, J.; Ge, G. L.; Brus, L. E. *J. Phys. Chem. B* **2002**, 106 (22), 5653–5658.

(31) Harfenist, S. A.; Wang, Z. L.; Alvarez, M. M.; Vezmar, I.; Whetten, R. L. *J. Phys. Chem.* **1996**, 100 (33), 13904–13910.

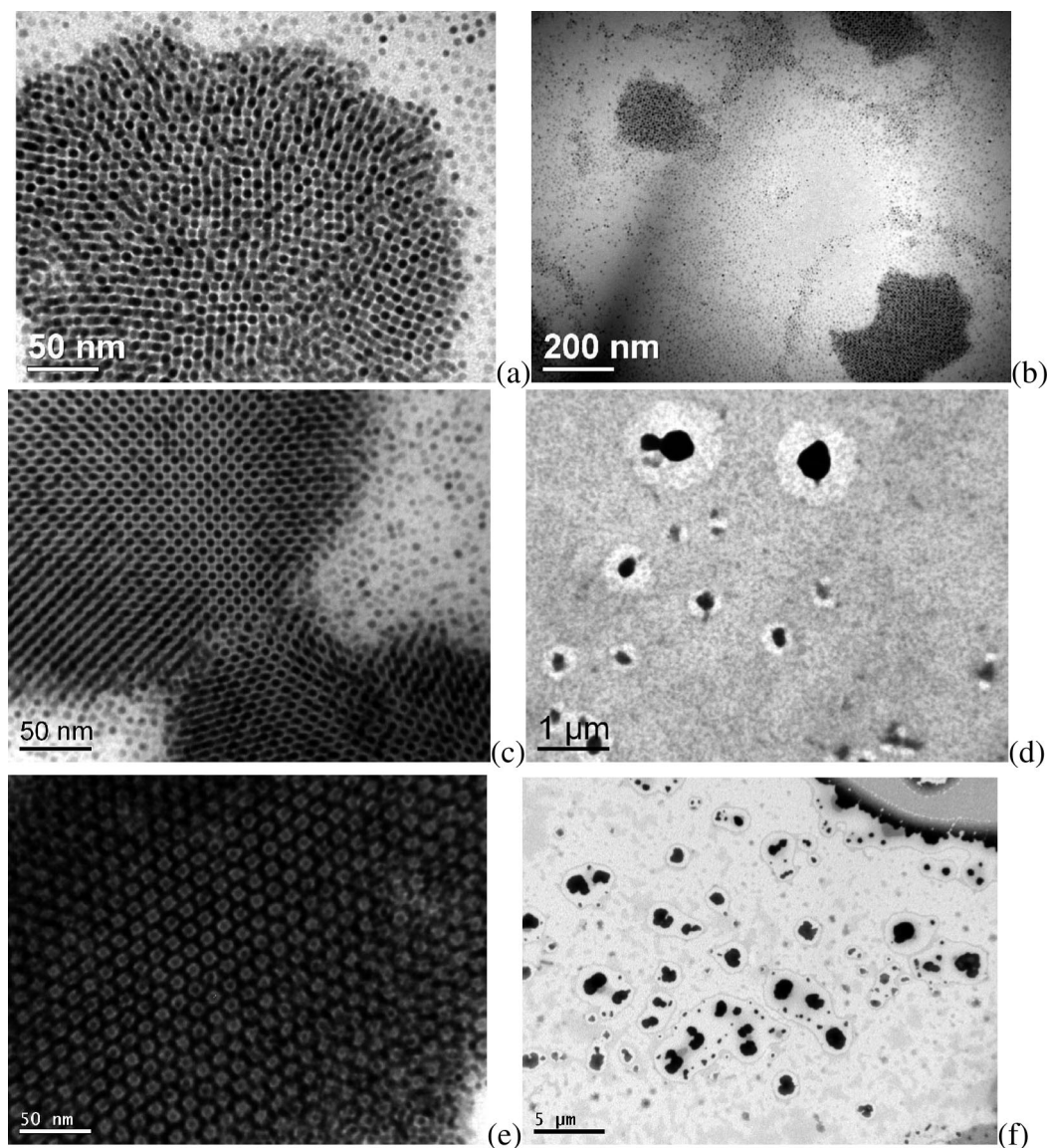


Figure 2. High (left column) and low (right column) magnification TEM images of CdSe-Au BNSLs of various sizes and symmetries formed from thiol/toluene solvent mixtures: (a, b) AB structure from 6.8 nm CdSe and 6 nm Au; (c, d) AB structure from 3.5 nm CdSe and 5.0 nm Au; (e, f) AB₅ structure from 6.8 nm CdSe and 5.8 nm Au.

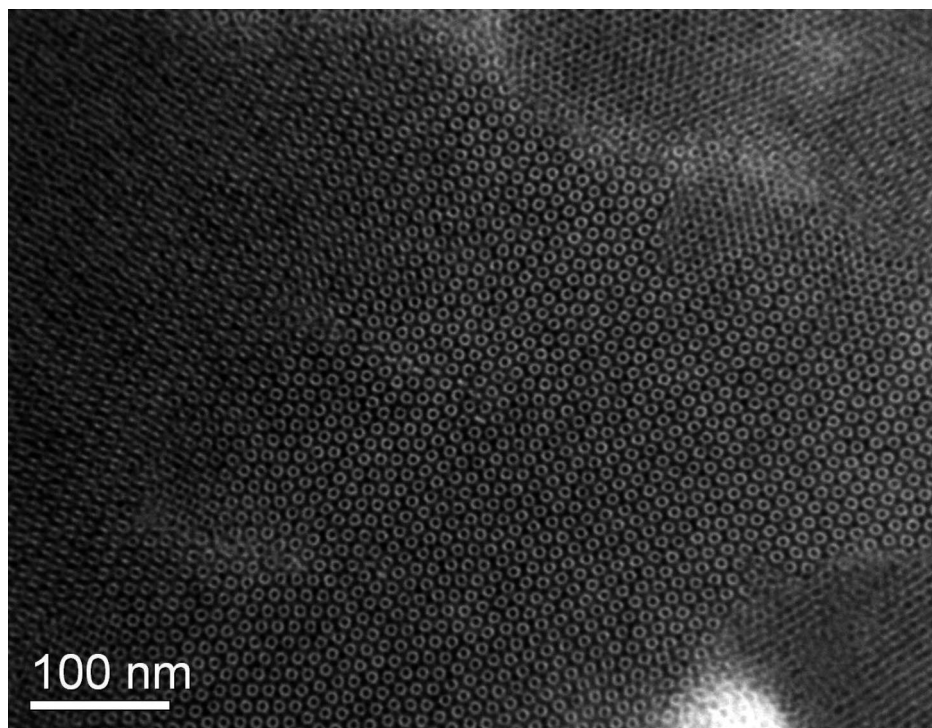
ring” patterns were also routinely observed (Supporting Information, Figure 2), due to a high nanoparticle flux toward the edge of the droplet during evaporation and due to fast evaporation of the low boiling point solvent (e.g., toluene).³² Correlation was not yet found between the coffee rings and the BNSL structure, suggesting that BNSL formation could be neither facilitated nor hindered by such rings. We observe that settling and ordering of nanoparticle assemblies requires a time scale longer than the coffee ring formation and that the deterministic factor for BNSL formation remains to be confinement of nanoparticles into a small enough volume of slowly evaporating high bp solvent, as opposed to a formation mechanism that supports a mechanism of BNSL formation at the edge-bound nanoparticle flux. Our current understanding of the drying process is summarized in Scheme 1.

The conditions optimized for the CdSe/Au binary nanoparticle system were found to be effective for differently

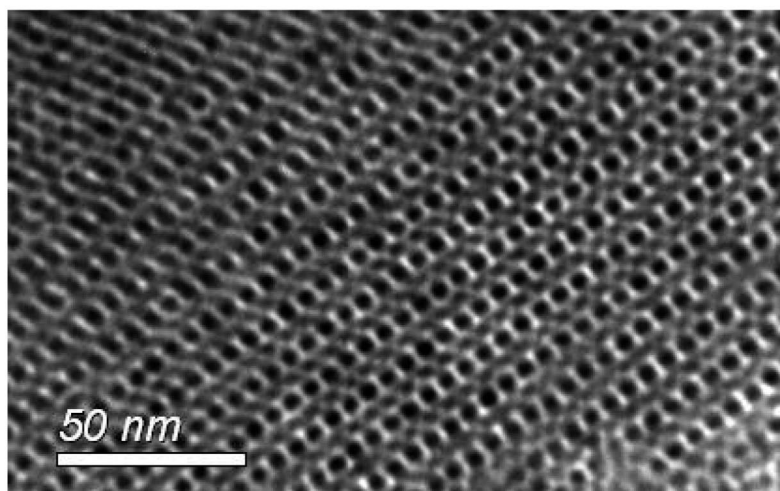
sized CdSe/CdSe systems as well. BNSLs were formed with thiol concentrations similar to those optimized for the CdSe/Au system. Two symmetries were obtained in this CdSe/CdSe (3.5 nm/5.5 nm) system: BNSLs with the structures AB and AB₅, obtained with a dodecanethiol-in-toluene concentration of 1.8% (Figure 3). We note that the optimized concentration of thiol can be applied to a variation of the binary systems and that changing the types of nanoparticles to CdSe only does not affect the outcome.

In conclusion, we fabricated Au-CdSe and CdSe-CdSe BNSLs in the presence of 1-dodecanethiol. The BNSL formation mechanism was investigated by studying the drying patterns of nanoparticles assemblies on amorphous carbon films. The influence of thiol was investigated under various concentrations to determine optimized conditions for guided assembly, for which relatively large ($>1 \mu\text{m}^2$) areas of superlattices could be routinely formed. Depending on appropriate selection of the radius ratio, AB or AB₅ binary structures of CdSe-Au nanoparticles were generated. The

(32) Deegan, R. D.; Bakajin, O.; Dupont, T. F.; Huber, G.; Nagel, S. R.; Witten, T. A. *Nature* **1997**, 389 (6653), 827–829.



(a)



(b)

Figure 3. (a) AB₅ and (b) AB structures from 3.5 nm CdSe and 5.5 nm CdSe nanoparticles.

optimized conditions for the CdSe/Au binary nanoparticle system was applied to and found to be equally effective for a binary mixture of CdSe/CdSe. We characterize CdSe-Au and CdSe-CdSe as additional systems to the library of possible binary nanoparticle superlattices.

Acknowledgment. This work was supported primarily by the MRSEC program of the National Science Foundation under award number DMR-0213574 and by the New York State Office

of Science, Technology, and Academic Research (NYSTAR). The research was also supported by NSF-CAREER award, DMR-0348938, and the U.S. Department of Energy, Office of Basic Energy Sciences, through grant DE-FG02-03ER15463.

Supporting Information Available: Addition TGA and TEM images (PDF). This material is available free of charge via the Internet at <http://pubs.acs.org>.

CM703117V